Research Journal of Applied Sciences, Engineering and Technology 5(22): 5159-5163, 2013
DOI:10.19026/rjaset.5.4259
ISSN: 2040-7459; e-ISSN: 2040-7467

Submitted: July 24, 2012 Accepted: September 08, 2012 Published: May 25, 2013

Research Article

Study in Cylindrical Coordinates of the Heat Transfer Through a Tow Material-Thermal Impedance

[1]A. Diouf, [1]I. Diagne, [1]M.S. Oul Brahim, [1]M.L. Sow, [2]F. Niang and [1]G. Sissoko
[1]Faculty of Science and Technology, University Cheikh Anta Diop in Dakar, BP 5005, Dakar-Fann, Senegal
[2]University Institute of Technology IUT/UT, University of Thies, Senegal

Abstract: We propose in this study a characterization of the temperature and of the heat flux density within a material tow disposed in cylindrical. The study is carried under dynamic frequency regime. By thermal-electrical analogy, the thermal impedance of the material is determined. The profiles of temperature curves, of heat flow density and thermal impedance allow us to appreciate the tow material behavior in insulation. The tow is made of plant fibers (sisal, jute, hemp).

Keywords: Dynamic frequency regime, thermal impedance, tow

INTRODUCTION

Ferent models for the study of heat transfer (finite medium or semi infinite) are proposed for the characterization of materials (Voumbo *et al*., 2010a). Measurement techniques allow us to determine the thermo physical parameters (thermal conductivity, thermal effusively, thermal diffusivity coefficient ...) (Voumbo *et al*., 2010b; Meukam *et al*., 2004).

We propose a study in cylindrical coordinates of heat transfer in a material of cylindrical shape, of finite dimensions with axial symmetry in dynamic frequency regime. The cylindrical system isolated such as water pipes simple or coaxial justifies the purpose of this study.

The profiles of the curves of temperature and heat flux density allow to highlight the behavior of heat through the material tow used as thermal insulation.

From the electrical analogy - Thermal (Jannot *et al*., 2009) the thermal impedance of the material is determined in cylindrical coordinates.

MATHEMATICAL MODELING

Diagram of the study: Figure 1 shows the tow material in cylindrical form. It is subjected at its base surfaces to stresses climate where the temperature varies in dynamic frequency regime. The coefficients of heat exchange at its faces and on the side face are attached.

Ta_1 and Ta_2 are the temperatures environmental, imposed in the direction (oz) respectively at the front and rear, under dynamic frequency regime.

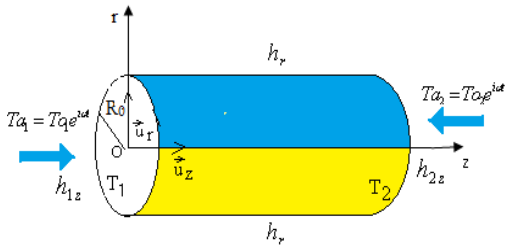

$0 \le r \le R_0$; $0 \le z \le H$; $R_0 = 0{,}02$m ; H = 0,03m

Fig. 1: Schematic of study design

- $T_{01} = T_{02} = 25°C$: maximum temperature of the environment
- The material is assumed to have an initial temperature Ti = 0°C
- ω Excitation frequency of temperature environmental

Expression of the temperature: Without source and heat sink, the heat equation is expressed:

$$\Delta T - \frac{1}{\alpha}\frac{\partial T}{\partial t} = 0 \quad (1)$$

Avec:

$$\alpha = \frac{\lambda}{\rho.C} \quad (2)$$

In cylindrical coordinates with axial symmetry, the temperature T is not dependent on the coordinateθ, the differential equation is:

Corresponding Author: G. Sissoko, Faculty of Science and Technology, University Cheikh Anta Diop in Dakar, BP 5005, Dakar-Fann, Senegal

$$\frac{\partial^2 T}{\partial r^2}+\frac{1}{r}\frac{\partial T}{\partial r}+\frac{\partial^2 Z}{\partial z^2}-\frac{1}{\alpha}\frac{\partial T}{\partial t}=0 \quad (3)$$

The solution of Eq. (3) under dynamic frequency regime, provided the conditions imposed in Fig. 1 and applying the method of separation of variables leads to the solution given by Eq.(4):

$$T(r,z,\omega,t)=\sum_{j=1}^{\infty}C_j J_0(\mu_j.r)\begin{bmatrix}A_j\sinh(\beta_j z)\\+B_j\cosh(\beta_j z)\end{bmatrix}e^{i\omega t} \quad (4)$$

With

$$J_0(\mu_j.r)=\frac{(r.\mu_j)^{k0}}{2^{k0}}\sum_{m=0}^{\infty}\left[\frac{(-1)^2.(r.\mu_j)^{2m}}{4^m.m!\,m!}\right] \quad (5)$$

$J_0(\mu_j.r)$ is a Bessel function with $K_0 = 0$
By applying the following boundary conditions:

$$\begin{cases}\lambda\left.\dfrac{\partial T}{\partial z}\right|_{z=0}=h_{1Z}\left[T(r,0,t)-T_{a1}\right] & (6)\\ -\lambda\left.\dfrac{\partial T}{\partial z}\right|_{z=H}=h_{2z}\left[T(r,H,t)-T_{a2}\right] & (7)\\ -\lambda\left.\dfrac{\partial T}{\partial z}\right|_{r=R_0}=h_r T(R_0,z,t) & (8)\end{cases}$$

We obtain expressions of the constants Aj and Bj from Eq. (6) and (7):

$$A_j=\frac{\begin{matrix}-h_{1z}To\left[\lambda\beta.coch(\beta.H)+h_{2z}\sinh(\beta.H)\right]\\+\lambda h_{2z}To_2\end{matrix}}{\begin{matrix}h_{1z}\begin{bmatrix}\lambda\beta_j J_0(\mu_j.r)\cosh(\beta.H)\\+h_{2z}J_0(\mu_j.r)\sinh(\beta.H)\end{bmatrix}\\+\lambda\begin{bmatrix}\lambda J_0(\mu_j.r)\sinh(\beta.H)\\+J_0(\mu_j.r)h_{2z}\sinh(\beta.H)\end{bmatrix}\end{matrix}} \quad (9)$$

$$B_j==\frac{h_{1z}h_{2z}To_1h_{2z}To_2\begin{bmatrix}\lambda\beta\ \cosh\ (\beta.H)\\+h_{2z}\sinh\ (\beta.H)\end{bmatrix}}{\begin{matrix}h_{1z}\begin{bmatrix}\lambda\beta J_n(\mu_j.r)\cosh\ (\beta.H)\\+h_{2z}J_n(\mu_j.r)\sinh\ (\beta.H)\end{bmatrix}\\+\lambda\begin{bmatrix}\lambda J_n(\mu_j.r)\sinh\ (\beta.H)\\+J_n(\mu_j.r)h_{2z}\sinh\ (\beta.H)\end{bmatrix}\end{matrix}} \quad (10)$$

Equation (8) possible to obtain the constant Cj

$$\lambda\mu J_1(\mu.R_0)-h_r J_0(\mu.R_0)=0 \quad (11)$$

Table 1: Eigen values

nj	2	7, 5	8,5	11, 5	14, 5	18
μ_j	66, 7	25	28, 3	38, 3	51, 6	60

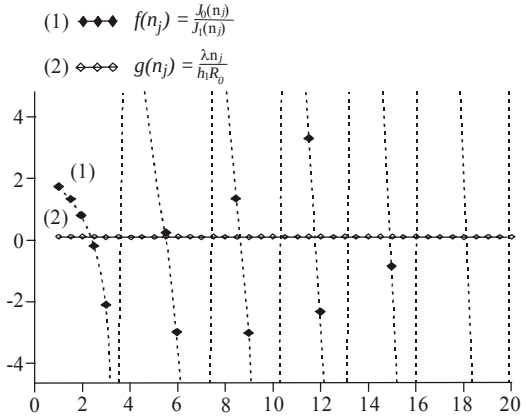

Fig. 2: Graphical determination of the Eigen values n^j

$$\frac{J_0(n_j)}{J_1(n_j)}=\frac{\lambda n_j}{h_r R_0} \quad (12)$$

$$n_j=R_0.\mu_j \quad (13)$$

Equation (12) gives the Eigen values nj (or μ_j) we determined graphically from Fig. 2:

We get a few Eigen values shown in Table 1.

At z = 0, we obtain:

$$T(r,0,t)=To=\sum_{j=1}^{\infty}C_j J_0(\mu_j r) \quad (14)$$

Of the normalization condition we obtain Cj:

$$C_j=\frac{\int_0^{R_0}rToJ_0\left(\dfrac{n_j r}{Ro}\right)dr}{\int_0^{Ro}rJ^2{}_0\left(\dfrac{n_j r}{Ro}\right)dr} \quad (15)$$

$$C_j=\frac{2ToJ_1(\mu_j Ro)}{\mu_j Ro\left[J^2{}_0(\mu_j Ro)+J^2{}_1(\mu_j Ro)\right]} \quad (16)$$

Expression of the heat flux density: The vector flux density of heat conduction is given by the following expression:

$$\vec{j}=-\lambda\ \vec{grad}T \quad (17)$$

$$\vec{J}=\vec{J}_r+\vec{J}_z \quad (18)$$

With

$\vec{J}_r$ = Vector density of heat flow in the direction (Or)
$\vec{J}_z$ = Vector density of heat flow in the direction (Oz)

The density of heat flow in both directions (Gold) and (Oz) are given respectively by:

$$\phi_r = \vec{J}_r . \vec{u}_r \quad (19)$$

$$\phi_z = \vec{J}_z . \vec{u}_z \quad (20)$$

The heat flux density is obtained by calculating global module:

$$\phi(r,z,\omega,t) = \sqrt{\left[\phi^2(r,z,\omega,t) + \phi^2(r,z,\omega,t)\right]} \quad (21)$$

$$\phi(r,z,\omega,t) = \lambda^2 \sum_{j=1}^{\infty} \left[\begin{array}{l} .C.e^{i\omega t}\left[(\mu_j J_1(\mu_j.r)\right) \\ \left[\begin{array}{l} A_j \cosh(\beta_j.z) + B_j \\ \sinh(\beta_j.z) \end{array} \right]^2 \end{array} \right]$$

$$+ \lambda^2 \sum_{j=1}^{\infty} \left[\begin{array}{l} C_j.e^{i\omega t} J_0(\mu_j.r) \\ \left[\begin{array}{l} \beta_j.A_j \cosh(\beta_j.z) \\ +\beta_j.B_j \sinh(\beta_j.z) \end{array} \right] \end{array} \right]^2 \Bigg\}^{\frac{1}{2}} \quad (22)$$

Expression of the thermal impedance: The thermal-electrical analogy (Ould Brahim *et al*., 2011) is used to define the thermal impedance from the relationship:

$$\Delta T = T_1 - T_2 = Z_{eq}.\phi \quad (23)$$

Z_{eq} = Thermal impedance of the material
ϕ = Heat flux density through the material
ΔT = Temperature variation between the front and rear faces

We obtain:

$$Z_T = \frac{\sum_{j=1}^{\infty} B_j C_j e^{i\omega t} - \sum_{j=1}^{\infty} \left[\begin{array}{l} C_j J_0(\mu_j.r) \\ \left[\begin{array}{l} A_j \sinh(\beta_j.z) \\ +B_j \cosh(\beta_j.z) \end{array} \right] \end{array} \right] e^{i\omega t}}{\phi} \quad (24)$$

RESULTS AND DISCUSSION

Evolution of temperature-following the direction (OZ): Figure 3 shows the curves of temperature changes in the direction (oz) in the tow material. We High light the influence of excitation fréquence.

The curves in Fig. 3 show the same profile. At the front, z = 0 m, the material absorbs heat and warms up (temperature rise). At inside the material, temperature decreases. when depth increases and tends to disappear

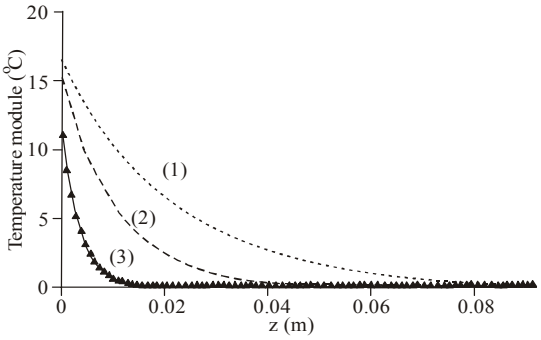

Fig. 3: Evolution of temperature in the tow material in function of depth z Influence of excitation r = 3/103m, h1z = 30 w/ (m2/°C), h2z =102 w/ (m2/°C), hr = 10-3 w/ (m2/ °C); t=1heure. (1) ω= 10 3 rad /s; (2) ω = 10-2 rad/s; (3) ω = 10 rad/s

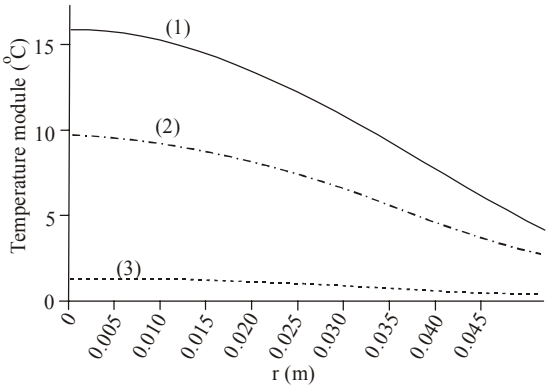

Fig. 4: Evolution of temperature in the material as a function of r. Influence of excitation frequency z = 102m; h1z = 30 w/ (m2/°C); h2z =102 w/ (m2/°C); hr = 10 3 w/ (m2/°C); t =1 heure; ω = 103 rad/s (1) ω =102 rad/s; (2) ω = 10 rad/s

when the thickness of the material becomes significant. The decrease in temperature is due to heat retention by the material. More than the storage capacity of energy by the material is important on low layer, the material is good thermal insulator.

The comparison of curves in Fig. 3 shows that the heat transmitted to tow material is even more important as the excitation frequency is low.

Following the radial direction (Or): The curves in Fig. 4 show the evolution of temperature in a radial direction (Or) contained in the plane of the circular base. The curves highlight the influence of excitation frequency.

The curves in Fig. 4 show the same profile. The maximum temperature module at r = 0, has a low variation for r <0.01 m and then decreases significantly in approaching the lateral side.

The heat transfer coefficient is assumed to virtually zero on the lateral side, the heat flow is imposed along

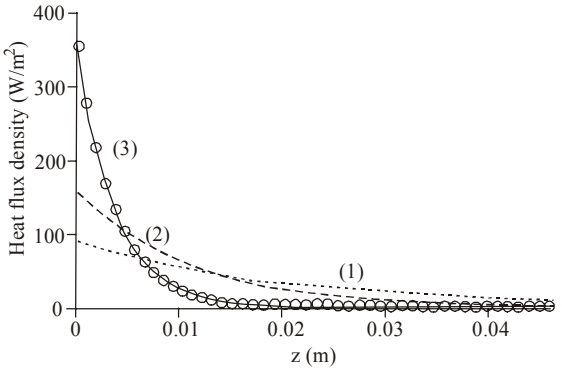

Fig. 5: Evolution of the heat flux density in the material as a function of depth z. Influence of excitation frequency, r = 102 m, h1z = 30 W/(m2/°C), h2z = 102 W/ (m2/°C), hr = 103 W/ (m2/°C); t =1heure/ (1) ω = 103 rad/s, (2) ω = 102 rad/s, (3) ω =10 rad/s

the direction (Oz) and we observe lateral heat losses and heat storage. We observe a drop in temperature of the order of 15°C relative to the temperature of the environment, for a thickness of about 0.03 m.

The comparison of the curves in Fig. 4 confirms the observations made in Fig. 3.

Evolution of the heat flux density:

Following the direction (Oz): The Fig. 5 shows the evolution of the density of heat flow through the tow material. The influence of the excitation pulse of the external environment is emphasized.

The curves in Fig. 5 show an overall reduction of the heat flux density when passing from the front, z = 0, within the material. For a thickness of about 0.03 m and in the study conditions, the tow material retains a significant amount of heat reflecting a good performance in thermal insulation.

The comparison of the curves in Fig. 5 shows that within the material, the heat retention is more important than the excitation frequency is important.

Following the radial direction: In Fig. 6, we present the evolution of the heat flux density through the material along the radius of the base of the cylinder. The influence of the excitation fréquence is Highlighted.

The heat flux density, maximum at r = 0, has a low variation for r <0.01 m and then decreases significantly when approaching the side. For r> 0.01 m, the behavior of thermal insulation tow material is considerable. These curves also show the importance of lateral heat losses relative to the direction of heat flow imposed.

The comparison of curves in Fig. 6 shows that the heat retention in tow material is even more important that the frequency excitation is high, curve (3); note that the low frequency excitation allows only low heat exchanges at the interface of the material, curve (1).

Thermal impedance of the tow material: The thermal impedance (Dieng *et al*., 2007) is used to characterize

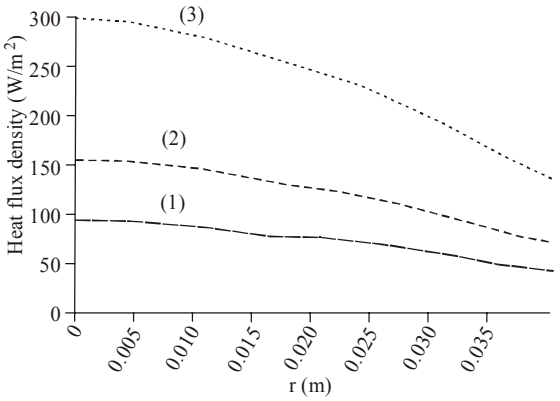

Fig. 6: Evolution of the heat flux density in the material in terms of r. Influence of excitation frequency, r = 10^2 m, h_{1z} = 30 W/(m^2/°C); h_{2z} = 10^2 W/(m^2/°C); hr = 10^{-3} W/ (m^2/°C); t = 1 heure. (1) ω = 10^3 rad/s, (2) ω = 10^2 rad/s, (3) ω =10 rad s^1

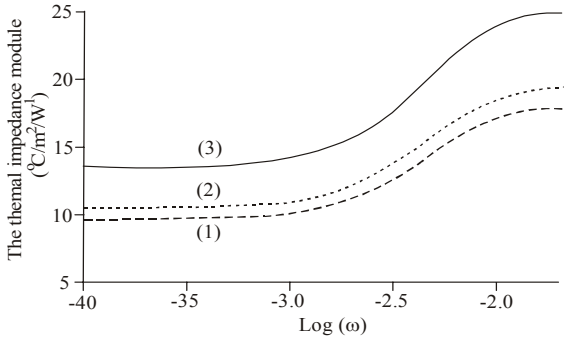

Fig. 7: Evolution of thermal impedance module. Influence of position along the radius r frequency z = 0,3m; h_{1z} =30 W/m^2/ °C^{-1} ; h_{2z} =10^2 W/ (m^2. °C), hr = 10^3 w/ (m^2. °C); t =1heure. (1) r = 0 m ; (2) r = 0,01 m ; (3) r = 0,02 m

the behavior of a thermal insulating material. The curves of Fig. 7 show the evolution of the thermal impedance of the tow material according to the excitation frequency of the temperature of the environment.

For a frequency band 10^4rad/s <ω<2, 1.10^2rad/s, the profile of the curves do not depend on the position r. The modulus of the impedance is constant for low frequencies, increases for intermediate frequency and reaches a plateau for high frequency. For a variation of temperature ΔT given between the two faces of the material, the increase in the modulus of the impedance corresponds to a decrease in the flow of heat through the material. This reduction in heat flow is partly due to the heat absorption by the material and on the other hand to a loss of heat by the lateral face.

CONCLUSION

The study of heat transfer in cylindrical coordinates has been proposed for tow material characterization.

From the mathematical model, the curves of change of temperature, heat flux and the dynamic impedance of the material have shown the optimum ranges of frequencies resulting in a high heat transfer.

The influence of heat transfer coefficient shows the need to control the external environment of material.

ACKNOWLEDGMENT

We thank all the authors cited in references; their work we are a very big contribution. We also thank the members of the international group of research renewable energy of laboratory of semiconductors and solar energy at the University Cheikh Anta Diop in Dakar.

REFERENCES

Dieng, A., L. Ould Habiboulahy, A.S. Maiga, A. Diao and G. Sissoko, 2007. Impedance spectroscopy method applied to electrical parameters determination on bifacial silicon solar cell under magnetic field. J. Sci., 7(3): 48-52.

Jannot, Y., A. Degiovanni and G. Payet, 2009. Thermal conductivity measurement of insulating materials with a three layers device. Int. J. Heat Mass Trans., 52: 1105-1111.

Meukam, P., Y. Jannot, A. Noumow and T.C. Kofan, 2004. Thermo physical characteristics of economical building materials. Constr. Build. Mater., 18: 437-443.

Ould Brahim, M.S., I. Diagne, S. Tamba, F. Niang and G. Sissoko, 2011. Characterization of the minimum effective layer of thermal insulation material tow-plaster from the method of thermal impedance. Res. J. Appl. Sci. Eng. Technol., 3(4): 337-343.

Voumbo, M.L., A. Wareme, S. Gaye, M. Adji and G. Sissoko, 2010a. Characterization of the thermophysical properties of kapok. Res. J. Appl. Sci. Eng. Technol., 2(2): 143-148.

Voumbo, M.L., A. Wareme and G. Sissoko, 2010b. Characterization of local insulators: Sawdust and wool of kapok. Res. J. Appl. Sci. Eng. Technol., 2(2): 138-142.